

# Fast control of the six phase asymmetric generator with the 3rd harmonic current injection

MAREK GOŁĘBIOWSKI

*Rzeszow University of Technology  
The Faculty of Electrical and Computer Engineering  
ul. Wincentego Pola 2, 35-959 Rzeszów, Poland  
e-mail: yegolebi@prz.edu.pl*

(Received: 26.11.2014, revised: 22.12.2014)

**Abstract:** In this paper the MTPA, MTPF, constant torque and constant flux control trajectories are presented. These trajectories are calculated for a 6-phase asymmetric inset-type SMPMSM generator with the assumption of a certain level of 3rd harmonic current injection. This injection technique increases the generator performance due to the cooperation of the fundamental and 3rd harmonic. The presented trajectories are used for fast control of the generator working in the gearless wind turbine system.

**Key words:** 6-phase asymmetric generator, third harmonic current injection, control trajectories, MTPA, MTPF

## 1. Introduction

This paper deals with the 6-phase asymmetric inset-type SMPMSM generator designed for operation in a gearless wind turbine system [1]. The generator under investigation is a low and variable speed machine with a large pole pair number. Such a machine has concentrated windings and therefore the third spatial harmonic component is not negligible [2-4]. This component is generated by the third harmonic of the windings specific electric loading. It appears as the third harmonic of the magnetic induction in the air gap and in stator phase fluxes. After transformation to the  $q, d$  coordinates it appears as the main component of the  $q_3, d_3$  coordinates. The third time harmonic of the stator currents forms this coordinate  $(q_3, d_3)$  [5]. The dimensions of the investigated machine can be found in [6].

## 2. Third harmonic current injection

Figure 1 presents the waveform of the generator phase current during its operation with 3rd harmonic current injection.

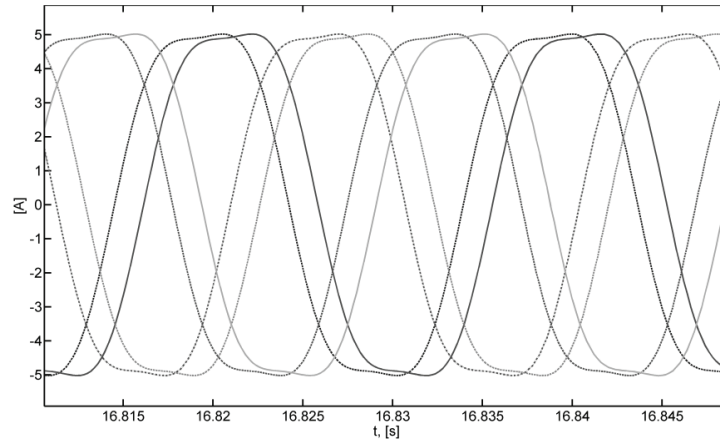


Fig. 1. The waveform of the stator phase currents with the 3rd harmonic current injection

The shape of the phase currents of the stator, as shown in Figure 1, is similar to a trapezoid. It demonstrates the participation of  $I_{q3}$ ,  $I_{d3}$  current components, which appears as the 3rd time-harmonic [7, 8]. The magnitude of the  $I_{q3}$  and  $I_{d3}$  current components is set according to (1).

$$\begin{aligned} I_{q3} &= k_{13} \cdot I_{q1}, \\ I_{d3} &= k_{24} \cdot I_{d1} \end{aligned} \quad (1)$$

The coefficients in (1) are set to  $k_{13} = -0.1$  and  $k_{24} = -0.3$ . The cooperation between fundamental and the third harmonics and the effect of the third harmonic is utilized. The selected coefficients ensure the existence of third harmonic currents in dependence on the first harmonic current, which gives the mutual enlargement of the torque and also the reduction of the torque pulsations [5].

### 3. Operating point selection

Figure 2 shows the control trajectories of a constant torque  $m_o$  (solid lines), a constant flux of  $\psi = U_{zn}/\omega_r$  (dashed lines), the maximum torque in relation to the current trajectory (MTPA – thick black line) and maximum torque in relation to the magnetic flux trajectory (MTPF – thick black line).

The line denoted with circles shows the maximum allowable current and limits the acceptable operating point area. The presented trajectories are calculated with the assumed injection of 3rd harmonic currents  $i_{q3} = k_{13} \cdot i_{q1}$ ;  $i_{d3} = k_{24} \cdot i_{d1}$ ; where  $k_{13} = -0.1$ ,  $k_{24} = -0.3$ .

The operating point is selected to provide the required torque. The best solution is to find the operating point on the MTPA trajectory (point 1 or 2). Point 1 is selected when the demanded torque is too large for the assumed value of rated current. In this situation a point on the current limit line must be chosen.

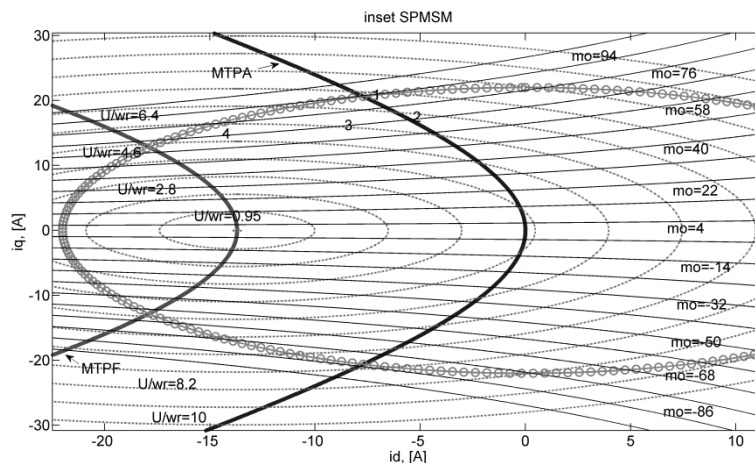


Fig. 2. The control trajectories of the machine SPMSM under test in the coordinates  $i_{q1}$ ,  $i_{d1}$  with the assumed injection of 3rd harmonic currents  $i_{q3} = k_{13} \cdot i_{q1}$ ;  $i_{d3} = k_{24} \cdot i_{d1}$ ; where  $k_{13} = -0.1$ ,  $k_{24} = -0.3$

Point 2 is selected when the demanded torque curve  $mo_{zad}$  intersects the MTPA curve within currents smaller than the rated current (in the acceptable operating point area). To accept these operating points the magnetic flux must first be checked. Its value at point 1 or 2 must be less than the currently maximal allowable value equal to  $U_{zn}/\omega_r$  (or than nominal flux). If this condition is not satisfied, the operating point 3 must be selected. This is the point of intersection of the demanded torque curve  $mo_{zad}$  (solid line) with the currently maximal allowable flux (dashed line). This is the point satisfying the conditions of achieving  $mo_{zad}$  and limiting the magnetic flux at the current as small as possible. However, the flux is at its limit in this point. Point 4, which is located on the constant torque trajectory  $mo_{zad}$ , can be considered as a working point at a lower flux (the number indicated on the dashed curve) but higher current. The choice between operating points 3 and 4, must be taken with the consideration of the power loss for heat in the stator resistance and the loss due to the magnetic flux in the stator iron. Point 4 can be located on the intersection of the constant torque with the MTPF trajectory or with the current limit line. In addition, the possible demagnetization of the permanent magnet should be prevented. For this purpose the current  $i_{d1}$  should be greater than its minimum permissible value  $i_{d1 \min}$ .

The presented control trajectories are tabulated for the discrete values of parameters (power, flux, torque). Figure 3 presents the voltages of the stator phases of the generator controlled with the presented method [3]. The disturbances of the voltages waveforms, observed in the form of voltage peaks, are caused by the rapid change of flux. These changes occur when the operating point is chosen from the different trajectory.

These disturbances can be reduced by approximating an average value between the trajectories. For the nearest two trajectories of constant flux  $U_{zn}/\omega_r$  (higher and lower than the current flux value) there are also points with a torque bigger and smaller than predetermined  $mo_{zad}$ . The first approximation is made between the curves of the constant flux, where the target value is the current flux  $U_{zn}/\omega_r$ . The approximation on the trajectory obtained this way is

made in relation to the torque in order to achieve  $m_{O_{zad}}$ . The obtained this way phase voltage waveforms are freed of described disturbances depicted in Figure 4.

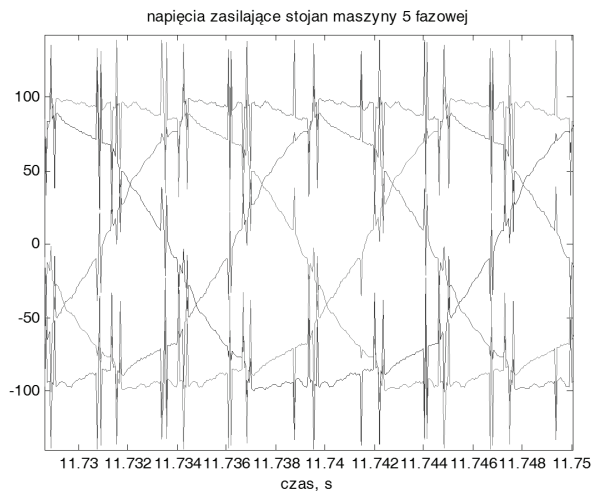


Fig. 3. Voltages of the stator phases of the generator controlled with presented method without use of the approximation between the trajectories

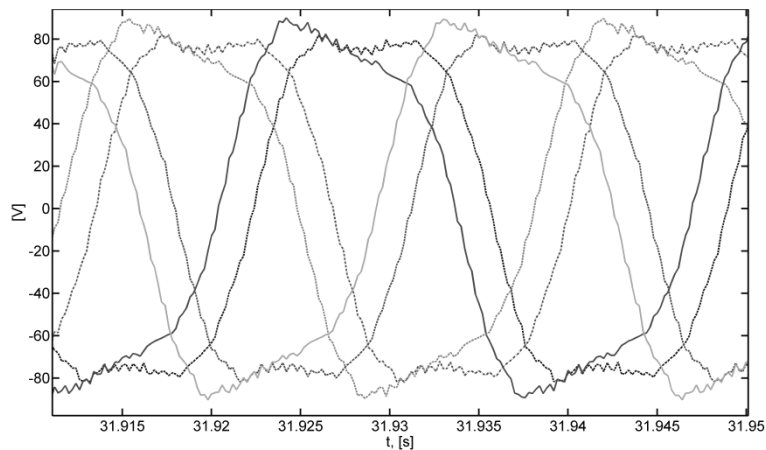


Fig. 4. Voltages of the stator phases of the generator controlled with presented method with use of the approximation between the trajectories

In the Figure 5 the dynamic waveforms of the tested system are shown. This waveforms illustrates how the system is trying to reach the set rotational speed  $\omega_{r_{zad}}$ . This speed depends on the measurements of the wind speed. Since the presented wind turbine system has no gears, it is a common speed for the generator and the turbine.

The tested system creates the electromagnetic torque (4), which would counteract a torque of the turbine (1) in order to obtain the desired speed of the turbine – generator system (3).

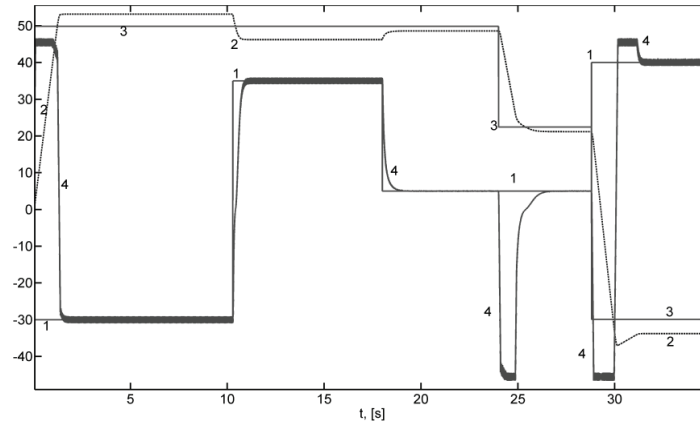


Fig. 5. Dynamic waveforms of the tested wind turbine-generator system: 1 – torque of the wind turbine, 2 – current speed of turbine-generator set, 3 – adjusted speed  $\omega_{r_{zad}}$  resulting from wind speed measurements, 4 – electromagnetic torque produced by the generator, opposing the torque generated by the wind turbine

#### 4. Attempts to reduce the electromagnetic torque ripples of the generator

The presented quick control system of the generator, based on precalculated characteristics with the use of the injection of the third harmonic currents, is characterized by the small electromagnetic torque pulsation. This is shown in Figure 6. In this figure, curve marked with number 3 presents the waveform of the actual electromagnetic torque of the machine. This waveform, in the following drawings, will be corrected in order to reduce the pulsation around its average value.

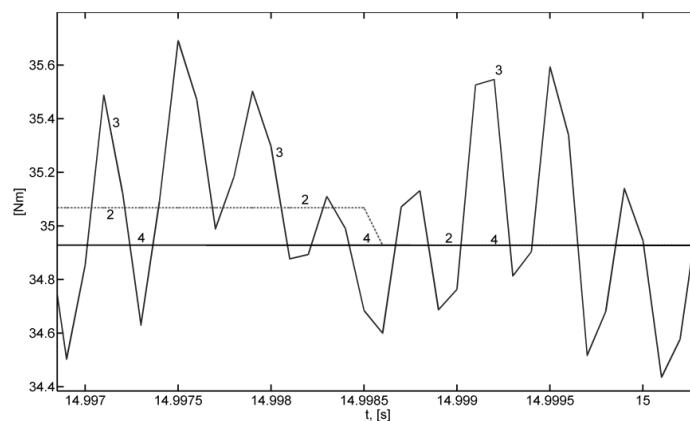


Fig. 6. Electromagnetic torque of the generator controlled with the characteristics browsing method: 3 – the actual electromagnetic torque, 2 – electromagnetic torque coming from the characteristics browsing, 4 – set torque resulting from the wind speed

The presented control method uses the averaged matrices of the inductance and permanent magnets coupled fluxes after transformation to the coordinates  $(q, d)$ . These matrices are calculated for different angular positions of the rotor, and then averaged. However, for specific positions of the rotor these matrices are different from their average values. These differences can be observed in Figure 7 [5, 6].

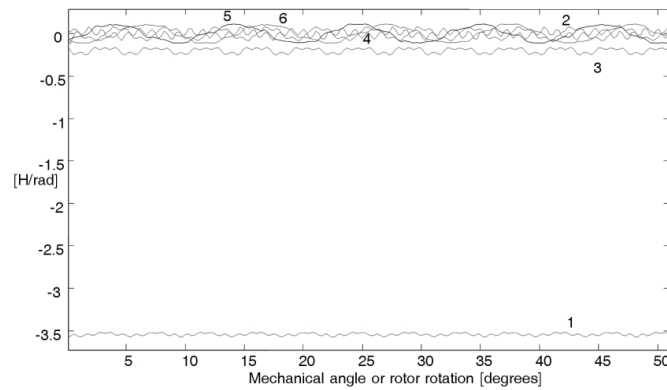


Fig. 7. Derivatives (with respect to mechanical angle) of the fluxes in the generator stator phases, induced by the permanent magnets as a function of the angle of rotation, after the transformation to the coordinates  $q, d$ : 1- $q_1$ , 2- $d_1$ , 3- $q_3$ , 4- $d_3$ , 5-01, 6-02 (before averaging)

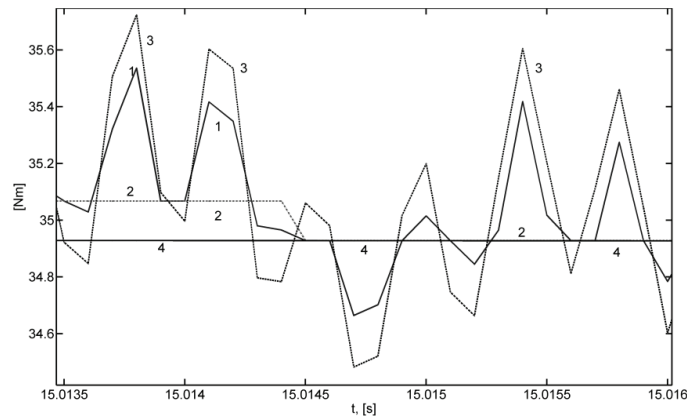


Fig. 8. Electromagnetic torque of the generator while reducing its pulsation through an additional correction of the  $i_{q1}$  current (maximal correction limited to 0.05 [A]): 1 – corrected electromagnetic torque (with smaller pulsation), 3 – actual electromagnetic torque before the correction, 2 – electromagnetic torque resulting from the characteristics (by the parameters averaged with respect to an angle of the rotation), 4 – set torque resulting from the wind speed and the current speed of the generator

Therefore, instead of the torque resulting from the control characteristic, which is indicated on Figure 6 with the number 2, the real torque curve marked with number 3 is obtained. The 3rd harmonic injection coefficients for this figures are, as before:  $k_{13} = -0.1$ ,  $k_{24} = -0.3$ . If the matrices of the inductance and permanent magnets coupled fluxes are known in the function

of the rotation angle, it is possible, with a little of calculation effort, to reduce the electromagnetic torque pulsation. This is shown in Figures 8 and 9.

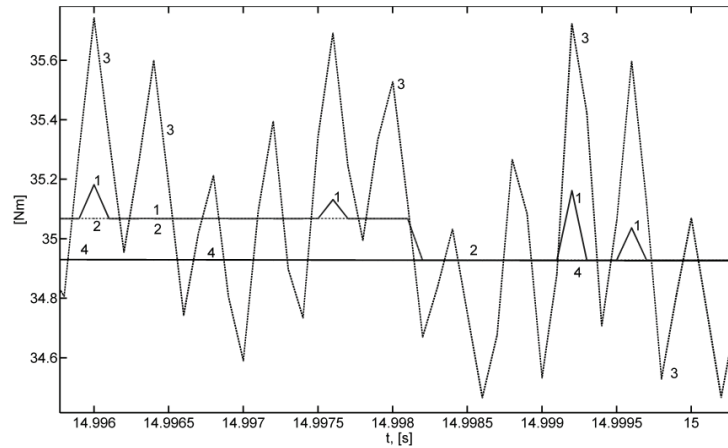


Fig. 9. Torque of the generator while reducing its ripples through an additional correction of the current  $i_{q1}$  (maximal correction limited to 0.15 [A]), marking as in Fig. 8

The reduction of the torque pulsation in Figure 8 is achieved with the third harmonic currents injection according to (1). In order to reduce those pulsation the formula for the electromagnetic torque  $m_o$  [6] is used:

$$m_o = [xx]' \cdot [m_{26}]' \cdot \{0.5 \cdot pma_{p_{sr}} \cdot [m_{26}] \cdot [xx] + pFm_{p_{sr}}\} \quad (2)$$

where:

$$[xx] = \begin{bmatrix} i_{q1} \\ i_{d1} \end{bmatrix}; \quad [m_{26}] = \begin{bmatrix} 1 & 0 \\ 0 & 1 \\ k_{13} & 0 \\ 0 & k_{24} \\ 0 & 0 \\ 0 & 0 \end{bmatrix} \quad (3)$$

In this formula, instead of the averaged (with respect to the angle of rotation) matrices of the transformed derivatives of inductance coefficients  $pma_{p_{sr}}$  and derivatives of the transformed permanent magnets fluxes coupled with the windings  $pFm_{p_{sr}}$  [6], the actual values (for a given rotor position) of the inductance derivatives matrix  $pma$  and derivatives of the coupled fluxes  $pFm$  matrix (before transformation) are used. With unchanged current  $i_{d1}$ , the corrected  $i_{q1}$ , so current value, providing the torque value equal to the value obtained from the characteristics (curve 2 of Fig. 8) is calculated. In addition, the change of this corrected current  $i_{q1}$  is limited (compared to the values got from the control characteristics) to predetermined value of 0.05 [A].

If the limiting  $i_{q1}$  correction value is increased to e.g. 0.15 [A], the torque pulsation are reduced more effectively. This is illustrated in Figure 9. However, in that case the demands on the maximum value of the stator phases voltage increases. The ability of the generator side converter to produce these voltages should be taken into consideration.

It should be noted that the presented method of the torque pulsation reduction, by taking into account fluctuations of matrices of the inductance derivatives and the coupled with the windings permanent magnet fluxes derivatives as a function of the angle of rotation, increase the requirements for the converter and for the control system as well. Generator's phase voltages corresponding to the waveforms in Figure 9, are shown in Figure 10.

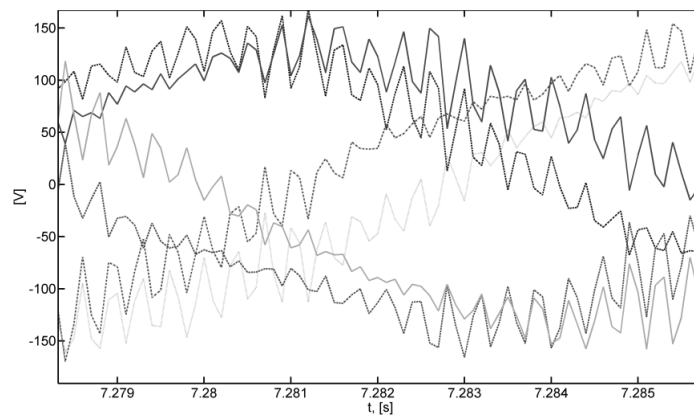


Fig. 10. Generator's phase voltages corresponding to the waveforms shown in Fig. 9, reducing the pulsation of the electromagnetic torque

To illustrate how the current coordinates, and therefore the current harmonics, associated with these coordinates, cooperate the calculations of the electromagnetic torque at different coefficients of 3rd current harmonic injection were conducted (4).

$$k_{13} = 0.4 \cdot \cos \alpha ; \quad k_{24} = 0.4 \cdot \sin \alpha, \quad (4)$$

where  $\alpha: 0 < \alpha < 2\pi$ .

This choice ensures a constant, equal to 0.4, module of the injection coefficients. The angle  $\alpha$  is a subsidiary angle, it is not the angle of the machine rotation. The electromagnetic torque was calculated from the formula (2), without the parameters averaging, for an exemplary position of the rotor defined by an electrical angle of  $297.6^\circ$  and for the currents  $i_{q1} = 3.866$  A,  $i_{d1} = -3.996$  A. That were the final values of the calculations presented in Figure 5. The torque value for different injection coefficients, expressed by the above formula, is shown in Figure 11.

Some of the points of the waveform presented in Figure 11 are distinguished with the injection coefficients  $k_{13}, k_{24}$ . The tested inset type SMPMSM machine has slots in the rotor in which the magnets are located. The size of these slots is 4.9 mm. From Figure 11 it can be seen, for which coefficients of the injection the harmonics cooperate ( $k_{13} = 0, k_{24} = -0.4$ ) and when there is counteraction ( $k_{13} = 0, k_{24} = +0.4$ ). For the coefficients of  $k_{13} = 0.4, k_{24} = 0$  and

$k_{13} = -0.4$   $k_{24} = 0$  there is no cooperation. Figures 8 and 9 show the possibility to reduce the electromagnetic torque ripples through additional improvement of the  $i_{q1}$  current component. For this method the matrices of the machine parameters in function of the rotation angle must be known. For the purpose of reducing the electromagnetic torque another method can be used. It involves the use of the appropriate coefficients of current injection and is presented in Figures 12 and 13. In this case the injection does not increase the electromagnetic torque, but is used to reduce its ripples.

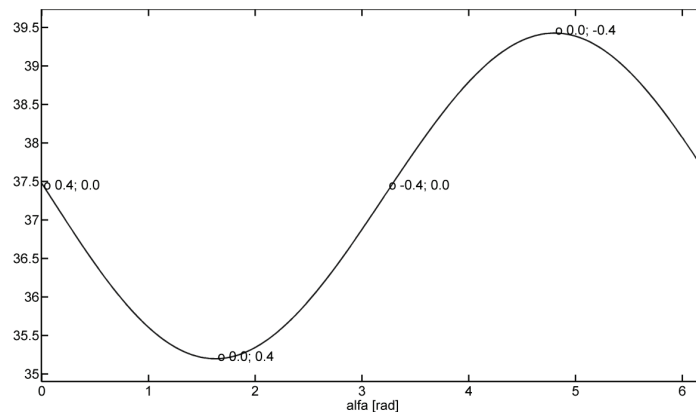


Fig. 11. Electromagnetic torque at different coefficients of injection  $k_{13}$ ,  $k_{24}$  expressed in dependence (4) ( $i_{q1}$  and  $i_{d1}$  are constant, and the values of  $i_{q3}$  and  $i_{d3}$  are changing:  
 $I_{q3} = k_{13} \cdot I_{q1}, I_{d3} = k_{24} \cdot I_{d1}$ )

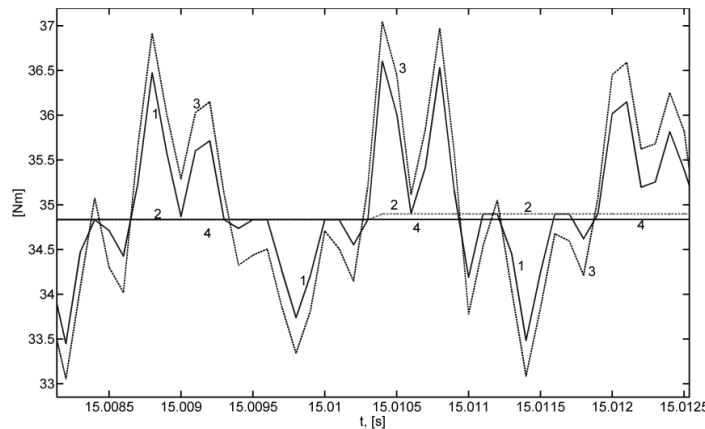


Fig. 12. The electromagnetic torques for the injection coefficients  $k_{13} = 0.4$ ,  $k_{24} = 0$  (then the third harmonic does not change the electromagnetic torque, Fig. 11): 1 – corrected electromagnetic torque ( $i_{q\text{popr}} = 0.05$  [A]), 2 – electromagnetic torque from the characteristics with averaged parameters, 3 – real electromagnetic torque without correction, 4 – set torque resulting from the wind speed and the current speed of the generator

The third harmonic injection coefficients, used in calculation of Figure 12, does not change the electromagnetic torque (there is no cooperation of the coordinates ( $q1, d1$ ) and ( $q3, d3$ ),

formed mainly by the first and the third harmonic of the current). The electromagnetic torque shows large fluctuations. The situation is similar for other factors of injection. The torque ripples of another characteristic occur for the injection coefficients, at which the basic and the third harmonic counteracts ( $k_{13} = 0, k_{24} = +0.4$ ). The torque pulsation harmonic of higher amplitude changed its frequency from 625 Hz (Fig. 12) to 120 Hz (Fig. 13).

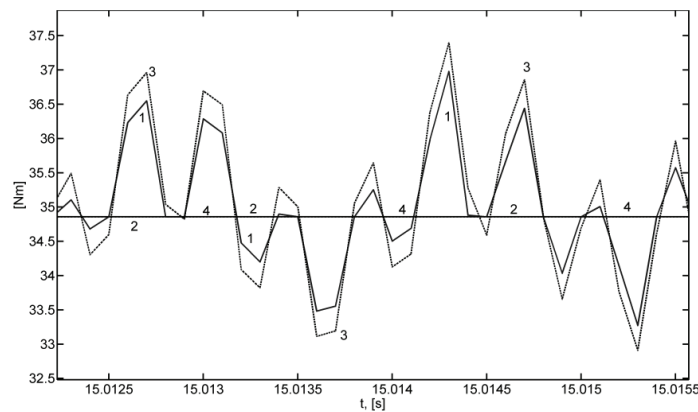


Fig. 13. The electromagnetic torques for the coefficients of the third harmonic currents injection  $k_{13} = 0, k_{24} = 0.4$  (the torques counteracts), marking as in Fig. 12

In both Figure 12 and Figure 13, the possibility to reduce the torque ripples with the method of the  $i_{q1}$  current correction (when  $|\Delta i_{q1}| < 0.05$  [A]; curve marked 1) was also examined.

Figure 11 shows the dependence of the electromagnetic torque, calculated for the selected time point (end of the calculation of Fig. 5), on the injection coefficients  $k_{13}, k_{24}$ . These coefficients are calculated according to (4). The electromagnetic torque consists of three components resulting from the action of the basic harmonic, the action of the third harmonic and from the cooperation between these harmonics. These components are present in the formula (2) and can be extracted by splitting the matrices  $pma_{P_{sr}}$  and  $pFm_{P_{sr}}$  into the submatrices of the size  $(2 \times 2)$  and  $(2 \times 1)$ . Submatrices, which are multiplied by the coordinates  $q1, d1$  define the action of the basic current harmonic, because it is an essential component of these coordinates. Similarly submatrices multiplied by the coordinates  $q3, d3$  represent an action of the third current harmonic as it is the main component of these coordinates. The non-diagonal submatrices represents the remaining component of the torque which is created by the cooperation of the first and the third coordinates.

The waveforms of these three components and the total value of the electromagnetic torque for the four selected (indicated in Fig. 11) injection coefficients, are illustrated in Figures 14-17. It should be noted that each of the three components of the electromagnetic torque contains as its part, a reluctance torque. It is generated by the inductance difference in the axis  $Lq$  and  $Ld$ , that is, for example, for the matrix  $ma_{P_{sr}}$  in formula (2), for successive components respectively by differences:  $ma_{P_{sr}}(1, 1) - ma_{P_{sr}}(2, 2), ma_{P_{sr}}(3, 3) - ma_{P_{sr}}(4, 4)$  and  $ma_{P_{sr}}(3, 1) - ma_{P_{sr}}(4, 2)$ .

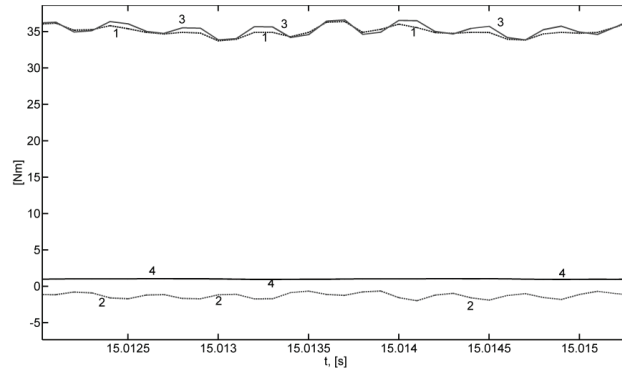


Fig. 14. Components of the electromagnetic torque for injection coefficients  $k_{13} = 0.4$ ,  $k_{24} = 0$  (no interaction of currents components): 1 – total torque, 2 – torque component only from the third harmonic currents ( $i_{q3}$ ,  $i_{d3}$ ) and from the fluxes  $F_{q3}$ ,  $F_{d3}$ , 3 – torque component only from the basic harmonic currents ( $i_{q1}$ ,  $i_{d1}$ ) and from the fluxes  $F_{q1}$ ,  $F_{d1}$ , 4 – the component from the cooperation of the currents ( $i_{q1}$ ,  $i_{d1}$ ) and ( $i_{q3}$ ,  $i_{d3}$ )

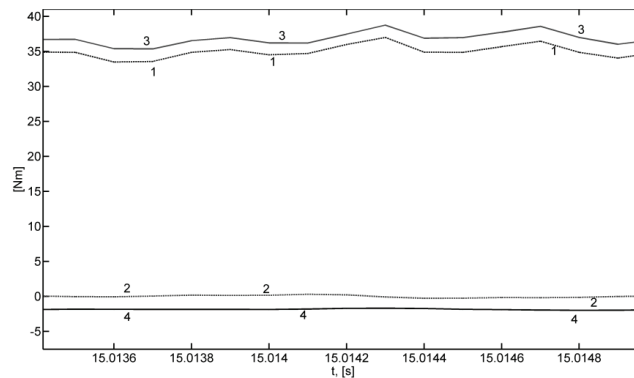


Fig. 15. Components of the electromagnetic for injection coefficients  $k_{13} = 0$ ,  $k_{24} = 0.4$ , (the basic and the third harmonic counteracts), marking as in Fig. 14

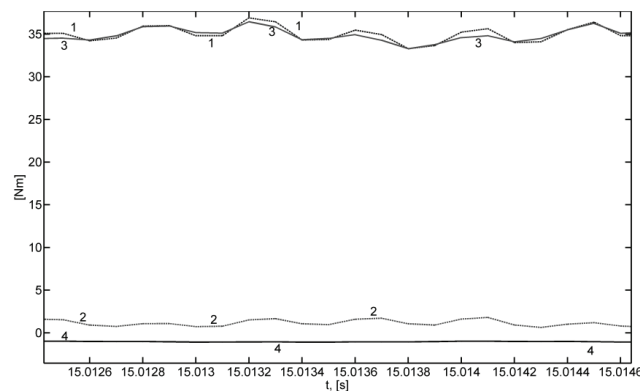


Fig. 16. Components of the electromagnetic torque for injection coefficients  $k_{13} = -0.4$ ,  $k_{24} = 0$  (no cooperation between the harmonics), marking as in Fig. 14

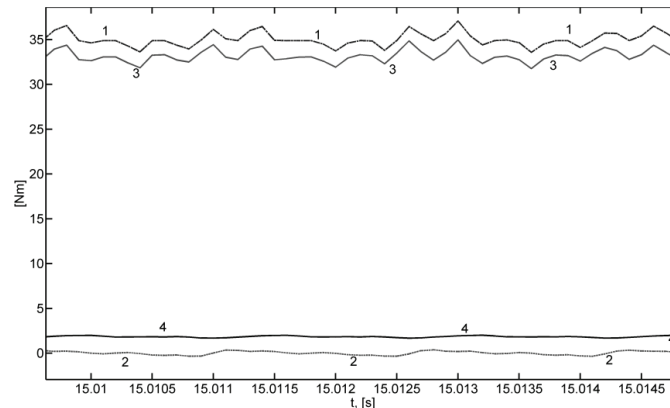


Fig. 17. Components of the electromagnetic torque for injection coefficients  $k_{13} = 0$ ,  $k_{24} = -0.4$  (the basic and the third harmonic cooperates), marking as in Fig. 14

The calculations presented in Figures 14-17 have been made with additional, previously described limited correction of the current  $i_{q1}$  ( $|\Delta i_{q1}| < 0.05$  [A], as shown in Fig. 8), which reduces the torque ripples, but requires knowledge of the matrix of derivatives of the coefficients of inductance and of derivatives of the flux as a function of the angle of rotation of the machine. Note the Figure 15, when there is a counteracting of the basic and the third harmonics. According to Figure 13, torque ripples are smallest at the time. Waveforms of Figures 14-17 illustrate the nature of the creation of the machine electromagnetic torque ripples components.

## 5. Conclusions

The generator control trajectories presented in Figure 2 are calculated with the assumption of the 3rd harmonic current injection. Level of this injection is determined by the  $k_{13}$  and  $k_{24}$  coefficients. The phase current of the generator has the trapezoidal shape which ensures the cooperation of the fundamental and 3rd harmonics [5-7]. Thanks to the use of calculated trajectories the control of generator is fast and accurate. It should be noted that, in the investigated 6 phase asymmetric generator, the 3rd harmonic current component flows in the neutral wire. Therefore, it is required that the generator power converter has the neutral connection [9].

There is a possibility of reduction of the torque pulsation by a slight correction of the  $i_{q1}$  component of the stator current. In this method the dependency of the inductance derivatives matrices and the derivatives of the permanent magnet fluxes coupled with the windings on the angle of rotation must be known. Another possibility of the torque pulsation reduction is the use of the of the  $q1, d1$  and  $q3, d3$  coordinates cooperation.

## References

- [1] Ayeahunie N.A., *MultiPhase Permanent Magnet Synchronous Generators for Offshore Wind Energy System*. Norwegian University of Science and Technology Department of Electric Power Engineering (2011).
- [2] Louis J.P., *Control of Synchronous Motors*. John Wiley&Sons (2011).
- [3] Xu1 G., Jian1 L., Gong1 W., Zhao W., *Quantitative comparison of flux-modulated interior permanent magnet machines with distributed windings and concentrated windings*. Progress in Electromagnetics Research 129: 109-123 (2012).
- [4] Liu J., Yang G., Li Y., Gao H., Su J., *Eliminating the Third Harmonic Effect for Six Phase Permanent Magnet Synchronous Generators in One Phase Open Mode*. Journal of Power Electronics 14(1): 92-104 (2014).
- [5] Tessarolo A., *Modeling and analysis of multiphase electric machines for high-power applications*. Scuola di dottorato di Ricerca in Ingegneria Industriale. Ciclo: XXII, Indirizzo Elettrotecnica (2011).
- [6] Mazur D., *Modeling and analysis of SPMSM machines in wind turbine applications* (in Polish). Oficyna Wydawnicza Politechniki Rzeszowskiej, Rzeszów (2013).
- [7] Louis J.P., *Control of Non-conventional Synchronous Motors*. John Wiley&Sons (2012).
- [8] Huang J., Kang M., Yang J., *Multiphase machine theory and its applications*. Electrical Machines and Systems (2008). ICEMS 2008. International Conference (2008).
- [9] Kaźmierkowski M., Sędkak M., Styński S., Malinowski M., *Hierarchical Control of Four-Leg Three-Level Grid-Connected Converter for RES*. Wybrane Zagadnienia Elektrotechniki i Elektroniki (WZEE, CD), pp. 10-18 (2013).